Hindawi
Journal of Nanomaterials
Volume 2022, Article ID 4888128, 11 pages
https://doi.org/10.1155/2022/4888128

Research Article

Impact of Swimming Gyrotactic Microorganisms and Viscous Dissipation on Nanoparticles Flow through a Permeable Medium: A Numerical Assessment

Sohail Ahmad,[1] Jihad Younis,[2] Kashif Ali,[3] Muhammad Rizwan,[1] Muhammad Ashraf,[1] and Mohamed A. Abd El Salam[4]

[1]*Centre for Advanced Studies in Pure and Applied Mathematics, Bahauddin Zakariya University, Multan 60800, Pakistan*
[2]*Department of Mathematics, Aden University, Khormaksar, PO Box 6014, Yemen*
[3]*Department of Basic Sciences and Humanities, Muhammad Nawaz Sharif University of Engineering and Technology, Multan 60000, Pakistan*
[4]*Mathematics Department, Faculty of Science, Al-Azhar University, Nasr-City, 11884 Cairo, Egypt*

Correspondence should be addressed to Jihad Younis; jihadalsaqqaf@gmail.com

Received 19 November 2021; Revised 18 December 2021; Accepted 27 December 2021; Published 18 January 2022

Academic Editor: Mohammad Rahimi-Gorji

In this paper, heat and mass transportation flow of swimming gyrotactic microorganisms (microbes) and solid nanoparticles under the viscous dissipation effect is investigated. The flow model PDEs are renovated with ordinary ones using suitable boundary layer approximations. The system governing the flow model dimensionless equations as well as boundary conditions is numerically treated with the SOR (successive over relaxation) technique. The flow, heat, and mass transport characteristics are examined against the prime parameters. A comparison is examined to be in a good agreement with the earlier results. It is found here that flow and thermal characteristics of the problem are substantially affected by the porous medium. The outcomes evidently point out that porous medium causes an enhancement in the skin friction and density of the motile microbes. Further, the rate of heat transport is devaluated at the surface of sheet due to viscous dissipation and elevated due to suction.

1. Introduction

An enhancement in heat transfer due to nanofluids is essentially required in various thermal systems. Nanofluids possess better thermal conductivity as equated to usual fluids. Several researchers interpreted the nanofluid flows under different assumptions. The flow phenomenon and thermal variations of unsteady radiative nanofluid flow induced by the magnetized spinning disk was investigated by Acharya et al. [1]. The presence of partial slips at the disk surface has been executed in this analysis. Salahuddin et al. [2] examined 3D stagnation point flow of hybrid nanofluid passed along a stretchable heated wavy cylinder under the impact of variable thickness and slip conditions. Shafiq et al. [3] determined the heat, mass, and motile microorganisms transfer rates in the magnetohydrodynamic (MHD) convective flow of a tangent hyperbolic material. A boundary layer flow of an incompressible Williamson fluid over a permeable radiative stretched surface was investigated by Shafiq and Sindhu [4]. Both electric and magnetic fields were taken into account. Imran et al. [5] interpreted the effects of melting phenomena and nonlinear thermal radiation in Cross-nanofluid bioconvection flow with motile microorganisms with a convective boundary over a cylinder. Brownian motion and thermophoresis diffusion were also taken into account in this mathematical model. Bilal et al. [6] presented a numerical simulation of microorganisms, carbon nanotubes (CNTs), and ferric oxide water-based hybrid

nanofluid flow induced by a wavy fluctuating spinning disc with energy propagation. The nanofluid was synthesized in the presence of CNTs and magnetic nanoparticulates.

Recently, the intention of research community has shifted towards the study of gyrotactic microorganisms' in nanofluid flows. A microorganism is a living being that can evolve, replicate, respond to stimuli, and have a structured order. In this way, any protists, animals, fungi, and bacteria will be an entity. These species can be categorized in various ways. Unicellular and multicellular animals are two essential groups. The microorganism is a much tiny living being that cannot be observed without an unaided eye. Algae, archaea, dust mite, and bacteria are all the examples of microorganisms. Taxes (locomotive behavior of microbes) may describe the microorganism's movement. Some microbes are electrotaxis, rheotaxis, aerotaxis, chemotaxis, phototaxis, and gyrotaxis. The swimming microbs show fixed movement because of the torque. The torque produced from viscous drag and gravity in a flow causes the motion of gyrotactic microorganisms. The necessary factors, oxygen for breathing, light for photosynthetic, and search of nutrients (food) force microorganisms to move.

Enhanced nanofluid constancy, microscale fraternization, increased mass transmission, and application in microvolumes are the benefits that are obtained by incorporating the mobile microbes into the nanoparticle suspension [7]. Nanofluids with microbes can be used in many biomicrosystems such as nanochips to determine the toxicity and cellulose optimization. It is also beneficial to use the nanofluids with microbes in enzyme biosensors and microfluidics such as micro volumes and micromixers powdered. Our findings may also increase microbial fuel cell performance. Furthermore, gyrotcatic microbes can enhance the stability of nanofluids in a flow [8]. A microbial-enhanced oil restoration often utilizes bioconvection mechanisms in order to retain the shift in permeability, as nutrients and organisms are poured in the oil-carrying layer [9].

In nanofluid flows, the influences of gyrotactic organisms have been deeply studied. The transmission of heat and mass in the flow of gyrotactic organisms and nanoparticles was scrutinized by Ramzan et al. [10]. This research contained viscous desperation with nonlinear thermal radiation, slip effects, and convective boundary values. As the values of Peclet and Lewis number raised, a decreasing trend in the density of motile microbes was observed. In an investigation on the flow of nanofluids consisting of gyrotactic microorganisms, Chakraborty et al. [11] noticed a decrease in the thermal transport volume, boundary layers thickness, and flux of motile microorganisms through the fluid medium by increasing the magnetic field factor whereas the absorption of nanoparticles improved. Tausif et al. [12] explained the flow of nanofluid including motile microbes and nanoparticles with numerous slip influences. To gain the essential results in polymer industry, the values of numerous slip parameters were escalated, due to which the properties of fluid like microorganisms' mass and flux rate or heat transference rate can be declined/improvised. Iqbal et al. [13] investigated the two-dimensional steady flow of nanofluid containing nanoparticles and gyrotactic microorganisms. The stagnation point flow of discursively striking nanofluid was included in this research. Atif et al. [14] explored that the density of motile microorganisms which was increased by the buoyancy ratio parameters but depreciated by the micropolar parameters. They integrated the influences of Joule heating and thermal radiation. The increasing effect of the density of microorganisms due to Peclet and Lewis numbers were investigated by Acharya et al. [15]. The numerical solutions were examined by Keller box method which marked the decreasing effect of the concentration of microbes due to elevation in values of the Peclet number. Waqas et al. [16] discussed some important properties such as Arrhenius energy activation, nonlinear radiation, and gyrotactic microorganisms in the flow of electrically conducted Maxwell nanofluid. In this study, bioconvection across the porous media due to microbes has also been discussed in detail.

Zuhra et al. [17] developed the mathematical model in which two nanoliquids (Williamson and Casson) were used in the flow and heat transfer within porous media upon its vertical solid surface against autocatalysis chemical reaction and gyrotactic microbes. In order to simplify the governing equations, nondimensional variables were used and the coupled ODEs were numerically solved using the homotopic analytic method (HAM). This study clarified how microorganism's density was reduced by the parameters (e.g., heterogeneous chemical reaction and porous media). Aziz et al. [18] have performed numerical work on the boundary layer flow of the bioconvective nanofluid over a horizontal plate embedded in porous media and claimed that the bioconvection parameters had a marginal effect on the movement of mobile microorganisms. Shaw et al. [19] employed a spectral relaxation technique to solve nonlinear differential equations describing the flow of gyrotactic motile organisms and nanofluid. This bioconvection flow was considered over a sphere plunged within a permeable medium (under the combined influence of MHD and viscous dissipation). Kuznetsov [20] described the uncertain behavior of nonoscillatory and oscillatory conditions for nanofluid flow containing oxytactic organisms, which led to density stratification because of oxytactic motile organisms or the distribution of nanoparticles. Sarkar et al. [21] erected a bioconvective fluid in a permeable medium which holds gyrotactic microorganisms over an expanding surface. Aurangzaib et al. [22] oriented, for Darcy-Brinkman porous medium, a detailed study of bioconvection nanofluid together with gyrotactic microorganisms over a convectively heated wedge. Kessler [23] described, almost for the first time, the concept of bioconvection through a porous medium.

One of the aims to present this study is to determine how much bioconvection due to gyrotactic microorganisms affect the flow through a permeable media in the coexistence of viscous dissipation. Even though literature is available on the work under consideration but still bioconvective flow

due to gyrotactic microbes and nanofluids under the influence of viscous dissipation through permeable media, specifically, over a nonlinear expanding/shrinking surface is not explored. The novel results of the present work, acquired by varying the preeminent parameters, are elaborated and illustrated with the help of graphs and tables.

2. Description of Physical Model

A steady flow of gyrotactic microorganisms and nanoparticles is considered within a permeable media. Viscous dissipation effect has also been taken in the energy equation. The velocity and the swimming path way of organisms are not influenced by the nanoparticles. However, volume fraction of nanoparticles, which is larger than 1%, can interrupt the motion of microorganisms. To attain the desired stability of bioconvection, a mixture of solid nanoparticles and microbes is added in the base liquid. An ambient concentration of microbes as well as ambient concentration and temperature of the fluid far away from the surface of sheet is represented by N_∞, C_∞, and T_∞ (see Figure 1).

The relevant equations of the problem, in case of porous media and viscous dissipation, may be composed as [24–27]

$$\frac{\partial v}{\partial y} + \frac{\partial u}{\partial x} = 0, \tag{1}$$

$$u\frac{\partial u}{\partial x} + v\frac{\partial u}{\partial y} = \upsilon\frac{\partial^2 u}{\partial y^2} + u_e\frac{\partial u_e}{\partial x} + \frac{\mu}{\rho k^*}(u_e - u), \tag{2}$$

$$u\frac{\partial T}{\partial x} + v\frac{\partial T}{\partial y} = \frac{\tau D_T}{T_\infty}\left(\frac{\partial T}{\partial y}\right)^2 + \tilde{\alpha}\frac{\partial^2 T}{\partial y^2} + \frac{\mu}{\rho c_p}\left(\frac{\partial u}{\partial y}\right)^2 + \tau D_B\frac{\partial C}{\partial y}\frac{\partial T}{\partial y}, \tag{3}$$

$$v\frac{\partial C}{\partial y} + u\frac{\partial C}{\partial x} = D_B\frac{\partial^2 C}{\partial y^2} + \frac{D_T}{T_\infty}\frac{\partial^2 T}{\partial y^2}, \tag{4}$$

$$v\frac{\partial N}{\partial y} + u\frac{\partial N}{\partial x} + \frac{1}{C_w - C_\infty}\frac{\partial}{\partial y}\left[N\left(\frac{\partial C}{\partial y}\right)\right]bW_c = D_n\frac{\partial^2 N}{\partial y^2}, \tag{5}$$

Here, y-axis is taken normal to the sheet having velocity component v, and x-axis is considered to be in the direction of flow having velocity component u. Moreover, the terms involved in the flow model equations such as D_T, $\tilde{\alpha}$, D_n, C_∞, bW_c, T, D_B, k^*, τ, c_p, C, υ, N, T_∞, and ρ represent the thermophoretic coefficient, thermal conductivity, diffusivity of microorganisms, ambient concentration, cell swimming speed, temperature of fluid, nanofluid heat capacity ratio, Brownian diffusion coefficient, Darcy permeability, specific heat constant, kinematic viscosity, microorganism concentration, concentration of fluid, ambient temperature, and density, respectively. The BCs (boundary conditions) at sheet surface and far away from sheet can be written as

$$y = 0\, N = N_w, u = cx^m, v = v_w(x), C = C_w, T = T_w, \tag{6}$$

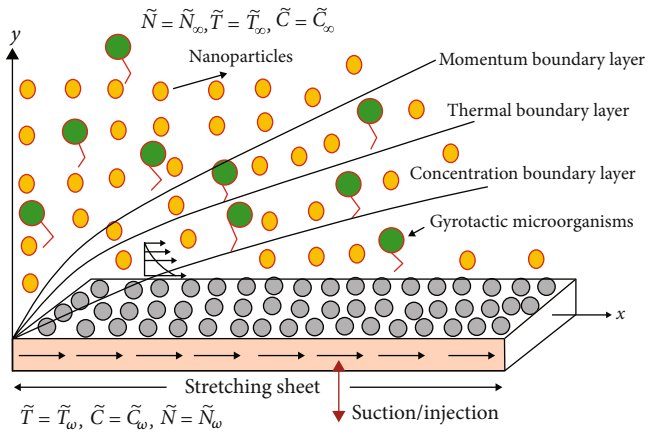

Figure 1: Geometry of the problem.

Table 1: Numerical data comparison of Sh_x for numerous S and $P_0 = \mathrm{Ec} = 0$ when $\Omega = 1, \mathrm{Pe} = 1, \mathrm{Sc} = 1, N_t = 0.5, \mathrm{Pr} = 6.2, \mathrm{Le} = 2, m = 1, N_B = 0.5, \alpha = -1$.

S	Sh_x		
	Literature results [24]	Literature results [34]	Present results
2.5	1.58189	1.58189	1.5802
3.0	1.82864	1.82864	1.8255
3.5	2.09161	2.09161	2.0866
4.0	2.36356	2.36356	2.3559
4.5	2.64078	2.64078	2.6298

$$y \longrightarrow \infty N = N_\infty, u = ax^m, C = C_\infty, T = T_\infty, \tag{7}$$

where v_w is the mass flux which describes suction (if $v_w > 0$) and injection (if $v_w < 0$). Whereas $u_e(x) = ax^m$ epitomizes ambient velocity and $u_w(x) = cx^m$ signifies stretching velocity, here, m is fixed ($m > 1$) which expresses the nonlinearity of shrinking/stretching sheet. Nondimensional variables are utilized (see Aini Mat et al. [28]) to convert partial differential equations (1)–(5) into ordinary differential equations:

$$\xi = \sqrt{\frac{a}{\upsilon}x^{m-1}}y, \psi = \sqrt{ax^{m+1}\upsilon}f(\eta), \phi(\eta) = \frac{C - C_\infty}{C_w - C_\infty}, G(\eta) = \frac{N - N_\infty}{N_w - N_\infty}, \theta(\eta) = \frac{T - T_\infty}{T_w - T_\infty}. \tag{8}$$

By using the coordinates of equation (8) in equations (2)–(5), the following nondimensional equations are achieved:

$$f''' = -\frac{1+m}{2}ff'' - P_0\left(1 - f'\right) + m\left(f'2 - 1\right), \tag{9}$$

$$\frac{1}{\mathrm{Pr}}\theta'' + N_b\phi'\theta' + \frac{1+m}{2}f\theta' + Ecf''^2 + N_t\theta'^2 = 0, \quad (10)$$

$$\phi'' = -\frac{N_t}{N_b}\theta'' - Le\frac{1+m}{2}\phi' f, \quad (11)$$

$$G'' + G' * \left(\frac{1+m}{2}\right) * f.Sc = Pe * \left[G' * \phi' + \left(\phi'' * (G+\Omega)\right)\right]. \quad (12)$$

The analogous boundary conditions (6) and (7) take the form:

$$\begin{aligned} \xi = 0: &\quad f = S = 1, f' = \alpha, \phi = 1, \theta = 1, \\ \xi \longrightarrow \infty: &\quad \phi \longrightarrow 0, f' \longrightarrow 1, \theta \longrightarrow 0, G \longrightarrow 0, \end{aligned} \quad (13)$$

where S denotes the injection/suction, α is the stretching (if $\alpha > 0$) or contracting (if $\alpha < 0$) of surface parameter. The other prevailing parameters involved in equations (9)–(12) are as follows:

$$\left.\begin{aligned} &\Omega = \frac{N_\infty}{N_w - N_\infty}, \mathrm{Le} = \frac{\nu}{D_B}, \mathrm{Ec} = \frac{u_e^2}{c_p(T_w - T_\infty)}, N_t = \frac{\tau D_T(T_w - T_\infty)}{\nu T_\infty}, \mathrm{Pe} = \frac{bW_c}{D_n} \\ &P_0 = \frac{\nu x}{k^* u_e}, \mathrm{Sc} = \frac{\nu}{D_n}, N_\mathrm{B} = \frac{\tau D_B(C_w - C_\infty)}{\nu}, \mathrm{Pr} = \frac{\nu}{\alpha}. \end{aligned}\right\}, \quad (14)$$

where Ω is the motile microbes' parameter, Le is the Lewis number, Ec is the Eckert number, N_t is the thermophoresis parameter, Pe is the Peclet number, P_0 is the porosity parameter, Sc is the bioconvection Schmidt number, N_B is the Brownian motion, and Pr is the Prandtl number

Further, dimensionless coordinates of engineering interest like skin friction, local density number of motile microbes, and Nusselt and Sherwood numbers may be defined as

$$\begin{aligned} \mathrm{Re}_x^{1/2} C_{fx} = f''(0), \mathrm{Re}_x^{-1/2} Nn_x = -G'(0), \mathrm{Nu}_x\ \mathrm{Re}_x^{-1/2} \\ = -\theta'(0), \mathrm{Re}_x^{-1/2}\mathrm{Sh}_x = -\phi'(0), \end{aligned} \quad (15)$$

where local Reynolds number is denoted as $\mathrm{Re}_x = U_e x/\nu$.

3. Numerical Solution

Now, we employ SOR method to construct an algorithm [29–33]. The order of equation (9) is reduced by one after modifying

$$s = f' = \frac{df}{d\xi}. \quad (16)$$

Now, equations (9) (12) have been transformed as

$$s'' + \frac{1+m}{2} * f * s' = -P_0(1-s) + m\left(-1 + s^2\right), \quad (17)$$

$$\frac{1}{\mathrm{Pr}}\theta'' + N_\mathrm{B}\phi'\theta' + \frac{1+m}{2}f\theta' + \mathrm{Ec}s'^2 + N_t\theta'^2 = 0, \quad (18)$$

$$\phi'' = -\frac{N_t}{N_\mathrm{B}}\theta'' - \frac{1+m}{2}\mathrm{Le}f\phi', \quad (19)$$

$$G'' + G'\frac{1+m}{2}f.\mathrm{Sc} = \mathrm{Pe}\left[G'\phi' + \phi''(G+\Omega)\right], \quad (20)$$

with boundary conditions:

$$\begin{aligned} &f(0) = 1, \quad G(0) = 1, \quad s(0) = \alpha, \quad \theta(0) = 1, \quad \phi(0) = 1, \\ &s(\infty) = 1, \quad G(\infty) = 0, \quad \theta(\infty) = 0, \quad \phi(\infty) = 0. \end{aligned} \quad (21)$$

Using finite differences, equations (17)–(20) take the following form:

$$s_i = \frac{1}{A_1}(B_1 s_{i+1} + C_1 s_{i-1} + D_1), \quad (22)$$

$$\theta_i = \frac{1}{A_2}(B_2\theta_{i+1} + C_2\theta_{i-1} + D_2), \quad (23)$$

$$\phi_i A_3 = (B_3 * \phi_{i+1} + C_3 * \phi_{i-1} + D_3), \quad (24)$$

$$G_i A_4 = (B_4 * g_{i+1} + C_4 * g_{i-1} - D_4), \quad (25)$$

whereas,

$$A_1 = 4 + 2h^2P_0 + 2h^2 ms_i, \quad B_1 = 2 + \frac{1+m}{2}hf_i,$$

$$C_1 = 2 - \frac{1+m}{2}hf_i, \quad D_1 = 2h^2 m + 2h^2 P_0,$$

$$A_2 = \frac{1}{\mathrm{Pr}}.(8), \quad B_2 = (4).\frac{1}{\mathrm{Pr}} + (\phi_{i+1} - \phi_{i-1})N_\mathrm{B} + h(1+m)f_i + \theta_{i+1}N_t - 2N_t\theta_{i-1},$$

$$C_2 = (4).\frac{1}{\mathrm{Pr}} - (\phi_{i+1} - \phi_{i-1})N_b - h(1+m)f_i + \theta_{i-1}N_t,$$

$$D_2 = \mathrm{Ec}\left(q_{i+1}^2 + q_{i-1}^2 - 2q_{i+1}q_{i-1}\right),$$

$$A_3 = 4, \quad B_3 = 2 + \frac{1+m}{2}\mathrm{Le}hf_i, \quad C_3 = 2 - \frac{1+m}{2}\mathrm{Le}hf_i,$$

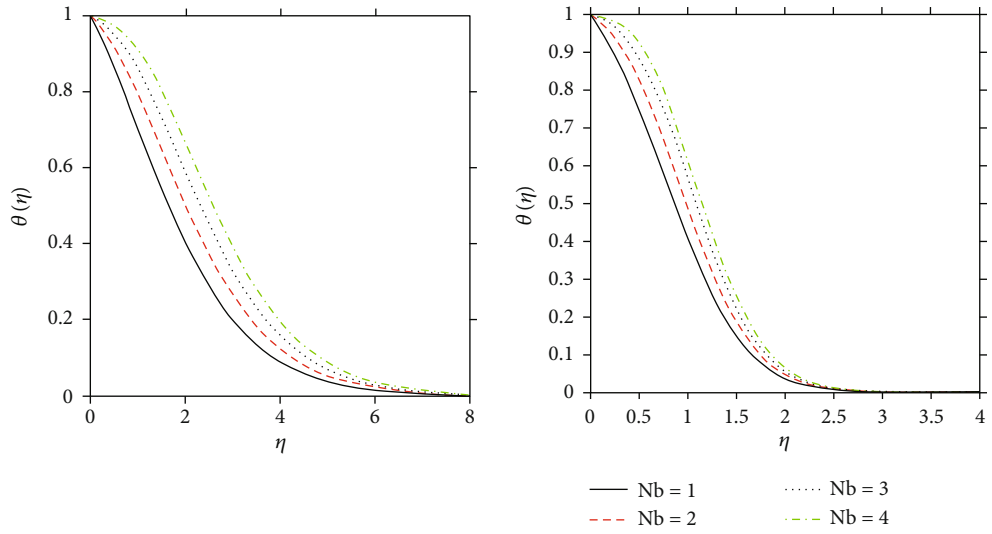

Figure 2: Profiles of temperature for various values of N_B when $N_t = \Pr = 1$, $\mathrm{Le} = m = 2$ and $\Omega = S = P_0 = \mathrm{Ec} = \mathrm{Pe} = 0$ [35].

Table 2: C_{fx}, Nu_x, Sh_x, and Nn_x for various m and P_0.

m	C_{fx}	Nu_x	Sh_x	Nn_x
2	1.5214	2.3092	1.7026	3.4770
3	1.8818	3.0710	2.0106	4.3890
4	2.2172	3.8447	2.2869	5.2761
5	2.5359	4.6277	2.5419	6.1460

$$D_3 = \frac{N_t}{N_B}(2).(-2\theta_i + \theta_{i+1} + \theta_{i-1}),$$

$$A_4 = 2(2) + \mathrm{Pe}.2(\phi_{i+1} - 2\phi_i + \phi_{i-1}),$$

$$B_4 = 2 + \frac{1+m}{2}h\mathrm{Sc}f_i - \frac{\mathrm{Pe}}{2}(\phi_{i+1} - \phi_{i-1}),$$

$$C_4 = 2 - \frac{1+m}{2}h\mathrm{Sc}f_i + \mathrm{Pe}.\frac{1}{2}(\phi_{i+1} - \phi_{i-1}),$$

$$D_4 = -\Omega.\mathrm{Pe}.2(\phi_{i+1} - 2\phi_i + \phi_{i-1}). \quad (26)$$

The succeeding approximation process is realistic to attain the numerical solution of the problem:

(a) To satisfy the BCs given in equation (21), the initial guesses are chosen for $\widehat{s}^{(0)}$, $\widehat{G}^{(0)}$, $\widehat{\theta}^{(0)}$, and $\widehat{\phi}^{(0)}$

(b) The Simpson's rule is applied to obtain $\widehat{f}^{(1)}$ from equation (16) which is used later in equation (22) to obtain $\widehat{s}^{(1)}$

(c) Finite difference discretization is utilized to simplify the system of equations (17)–(20), and then, the SOR method is employed to solve the resultant system of equations (22)–(25).

Table 3: Effect of porosity parameter P_0 on C_{fx}, Nu_x, Sh_x, and Nn_x when $Ec = 0$.

P_0	C_{fx}	Nu_x	Sh_x	Nn_x
0	1.4579	6.0947	-2.0467	1.7118
1	1.5647	6.0932	-2.0359	1.7209
10	2.2802	6.0881	-1.9808	1.7693
100	5.4378	6.1034	-1.8944	1.8601
200	7.4044	6.1172	-1.8816	1.8809
300	8.8924	6.1266	-1.8778	1.8903
400	10.1262	6.1335	-1.8765	1.8959
500	11.1948	6.1389	-1.8762	1.8996

Table 4: Effect of porosity parameter P_0 on C_{fx}, Nu_x, Sh_x, and Nn_x when $\mathrm{Ec} = 0.5$.

P_0	C_{fx}	Nu_x	Sh_x	Nn_x
0	1.4579	5.1070	-1.0654	2.1778
1	5647	5.0243	-0.9738	2.2253
10	2.2802	4.4522	-0.3544	2.5413
100	5.4378	1.8497	2.3339	3.8536
200	7.4044	0.2681	3.9307	4.6068
300	8.8924	-0.8888	5.0917	5.1458
400	10.1262	-1.8177	6.0212	5.5727
500	11.1948	-2.5984	6.8011	5.9278

(d) After the approximations $\widehat{G}^{(1)}$, $\widehat{s}^{(1)}$, $\widehat{\phi}^{(1)}$, and $\widehat{\theta}^{(1)}$ are obtained, the process is repetitive until the functions $\{\widehat{s}^{(k)}\}$, $\{\widehat{\phi}^{(k)}\}$, $\{\widehat{\theta}^{k}\}$, and $\{\widehat{G}^{(k)}\}$ converge

(e) When the following inequality is fulfilled, then, the procedure of calculations is stopped:

Table 5: Nu_x for variousPr, Ec, and N_t.

Pr	Nu_x	Ec	Nu_x	N_t	Nu_x
1	1.2460	1	1.8295	0.4	2.0968
3	2.0484	2	0.8724	0.8	1.4346
5	2.4904	3	-0.0987	1.2	0.9769
7	2.7936	4	-1.0842	1.6	0.6604

Table 6: Sh_x for various N_B and Le.

N_B	Sh_x	Le	Sh_x
0.2	0.1621	0.10	-1.0528
0.3	1.7101	0.15	-0.9038
0.5	2.8656	0.20	-0.7631
0.8	3.3985	0.25	-0.6315

Table 7: Nn_x for several Ω, Pe, and Sc.

Sc	Nn_x	Pe	Nn_x	Ω	Nn_x
0.2	0.9194	1	3.5318	1.0	3.3776
0.4	1.2851	2	4.3412	1.5	3.5060
0.6	1.6286	3	5.1730	2.0	3.6343
0.8	1.9588	4	6.0156	2.5	3.7627

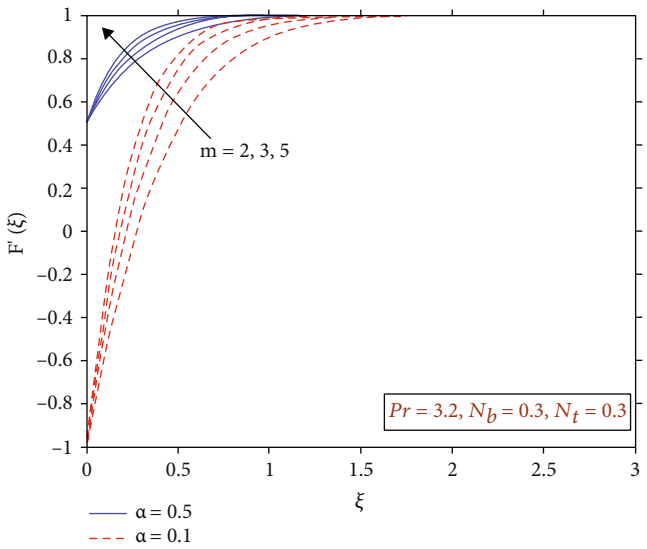

Figure 3: $F'(\xi)$ for various values of m and α.

$$\max\left(\left(\left\|\widehat{\phi}^{(k+1)}-\widehat{\phi}^{(k)}\right\|_{L_2}\right),\left(\left\|\widehat{G}^{(k+1)}-\widehat{G}^{(k)}\right\|_{L_2}\right)\right)<\mathrm{TOL}_{\mathrm{iter}},$$
$$\max\left(\left(\left\|\widehat{f}^{(k+1)}-\widehat{f}^{(k)}\right\|_{L_2}\right),\left(\left\|\widehat{\theta}^{(k+1)}-\widehat{\theta}^{(k)}\right\|_{L_2}\right)\right)<\mathrm{TOL}_{\mathrm{iter}} \quad (27)$$

We have taken value of TOL_{iter} as 10^{-11} in all the calculations performed here.

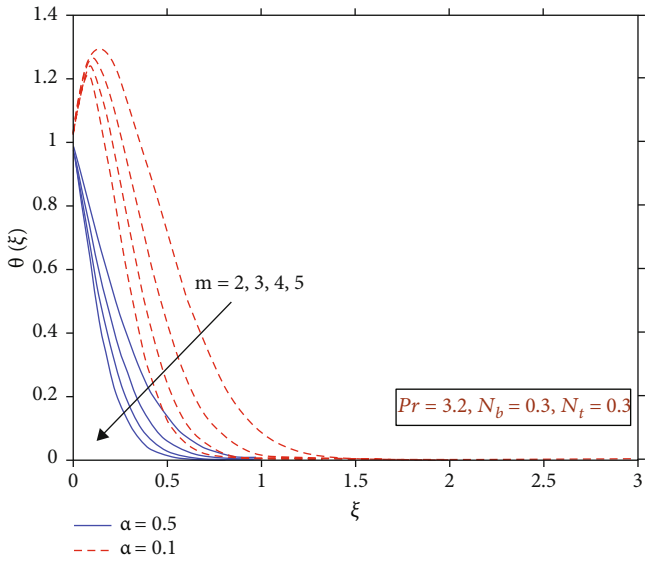

Figure 4: $\theta(\xi)$ for various values of m and α.

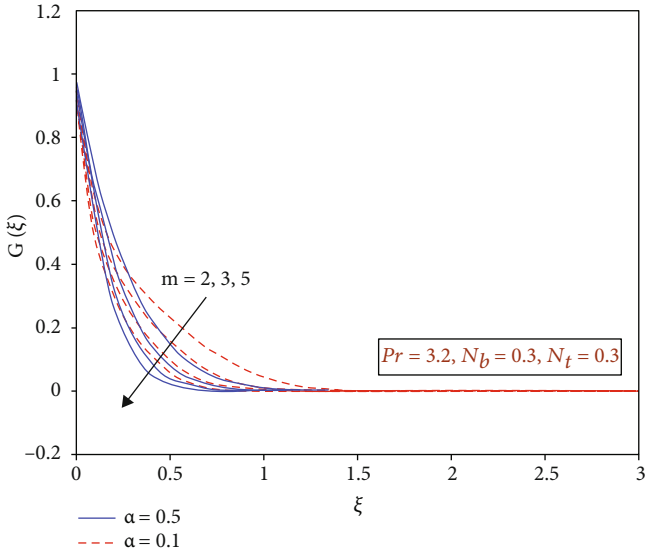

Figure 5: $G(\xi)$ for various values of m and α.

3.1. Comparisons and Code Validation. The simulation results are associated with the previously accomplished results (Table 1). The present results are in good contact with the previous ones. This evaluation approves the correctness of our code. Table 1 also designates that the local Sherwood number increases by escalating suction parameter sS.

The numerical data is selected from the available literature to associate our graphical outcomes with the existing ones (see Figure 2). Results are compared in the absence of porosity as well as bioconvection parameters. The comparison is in good contact with the literature results. The impact of Brownian motion parameter N_B is to promote the temperature $\theta(\eta)$ in the flow regime.

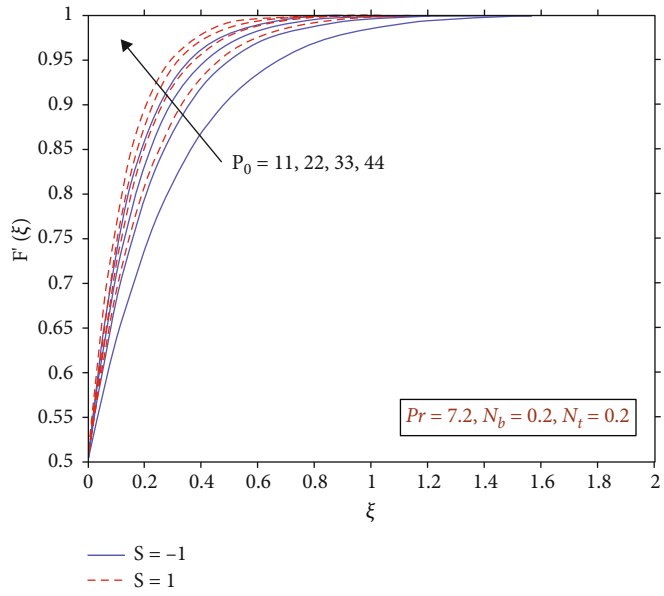

Figure 6: $F'(\xi)$ for various values of P_o and S.

4. Results and Discussions

In this section, numerical results are discussed with the help of physical interpretations. The system of equations (17)–(20) is a numerically tackled subject to boundary conditions (21) for distinct parameters. The SOR method is utilized to attain the numerical solutions. The motile microbe's density distribution $G(\xi)$, temperature $\theta(\xi)$, velocity $F'(\xi)$, and concentration $\phi(\xi)$ exhibit asymptotic expression for the estimated step size ξ. Mass and heat transport attributes can be analyzed by selecting several estimation values to the prime parameters, instead of utilizing unique field measurements and fluid characteristics. In this way, the parametric values should be modified for the particular applications of the work (Ahmad et al. [36–38]). Thus, we choose several values of the preeminent parameters such as $P_0 = 0.6$, Sc = 1.5, Ec = 0.5, Le= $2\Omega = 0.2$, $S = 1$, $Pe = 0.4$, $m = 2$, and $\alpha = 0.5$ otherwise specified.

Table 2 depicts that the density of local motile microbes and the skin friction are enhanced as the values of constant m increased positively; also, the same behavior is noticed for Nu_x and Sh_x.

Table 3 elucidates the effect of dimensionless porosity parameter P_0 on the physical quantities. The rates of heat and mass transfer are not significantly affected by the porosity of the medium which is due to the fact that the concentration and energy equation do not involve the porosity parameter. Moreover, only substantial change is noticed in shear stress. It may be due to the presence of P_0 (porosity parameter) in dimensionless momentum equation. As the pore size of the medium is larger than size of the microorganisms, so microbes' movement is not influenced by the flow through porous media. The structure of the gyrotactic microorganisms is not influenced by the permeable media having much smaller permeability (or high porosity). The dilute suspension, for which bioconvection takes place, may disturb the desired concentration in the presence of porous media having low porosity (or very small pores). It is noticed here that an increment in the porosity of the medium provides better solutions for bioconvection parameters as compared to smaller porosity. It is worth mentioning here that the density of microorganisms is more stable when porosity is large.

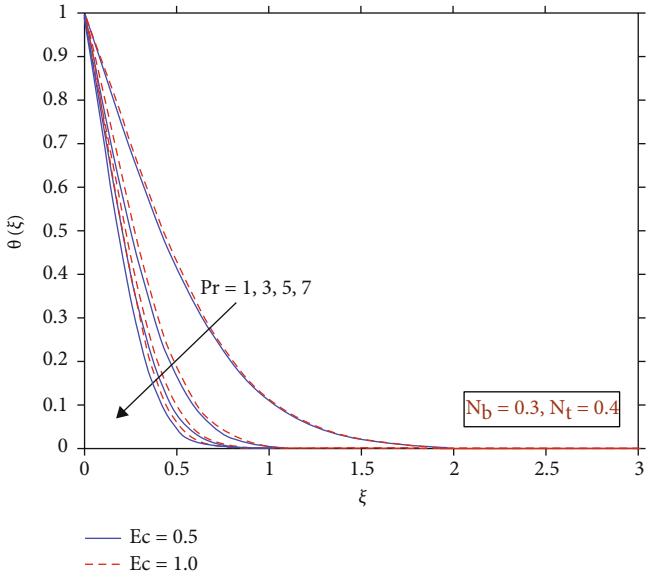

Figure 7: $\theta(\xi)$ for various values of Pr and *Ec*.

Now, if we increase the values of Eckert number (e.g., Ec = 0.5) then no change in skin friction is observed. It is noticed here that an increment in Ec leads to a significant decrease in heat transport rate, and it tends to increase the mass transport rate as well as density of the motile microbes

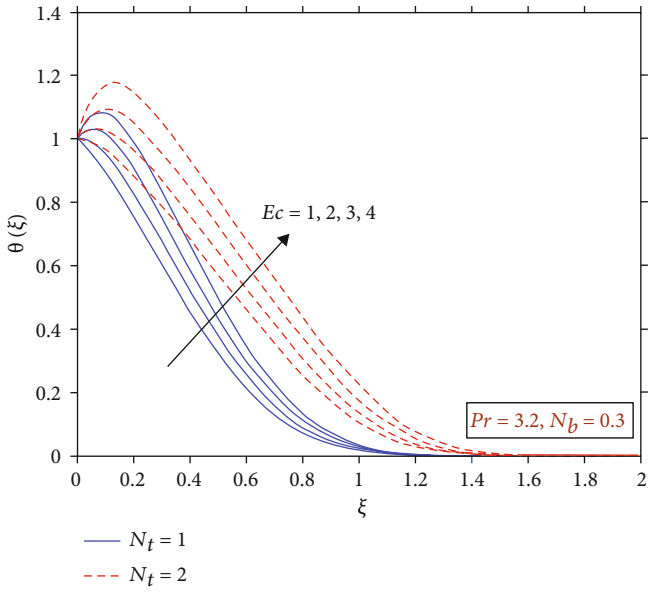

Figure 8: $\theta(\xi)$ for various values of Ec and N_t.

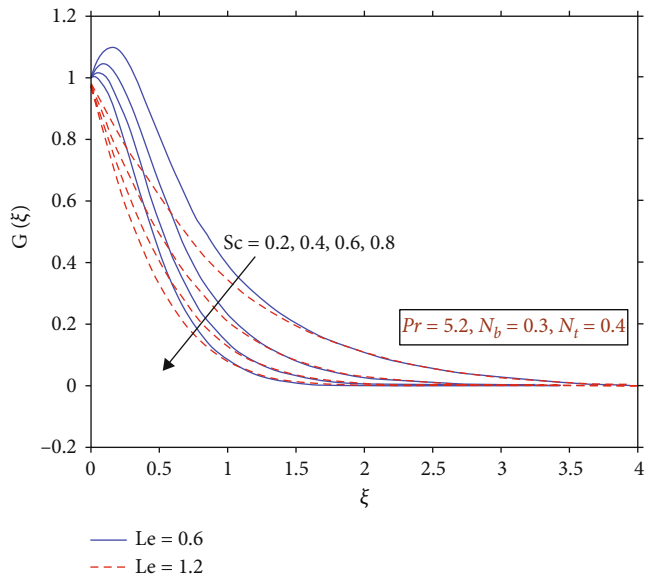

Figure 9: $G(\xi)$ for various values of Sc and Le.

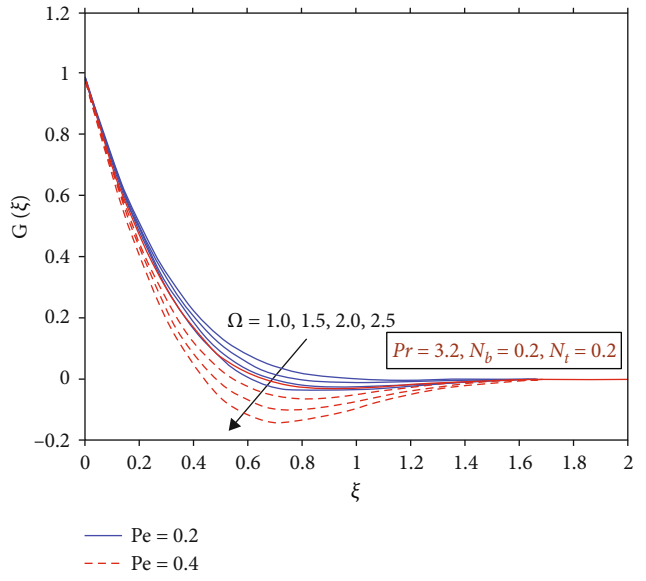

Figure 10: $G(\xi)$ for various values of Ω and Pe.

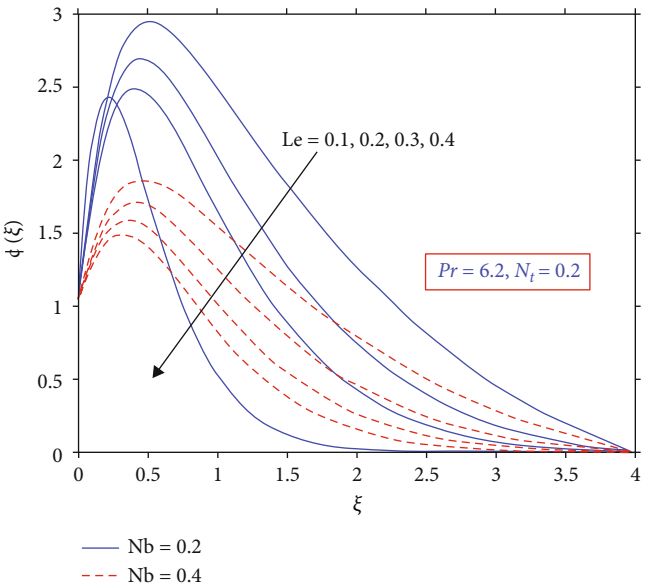

Figure 11: $\phi(\xi)$ for various values of Nb and Le.

(see Table 4). However, viscous dissipation does not affect the bioconvection through porous medium, and the density Nn_x enhances with viscous dissipation effect.

The rates of heat transportation for various values of Pr, Ec, and N_t are provided in Table 5. This table demonstrates the fact that the thermophoresis and viscous dissipation effects tend to decrease the rate of heat transportation whereas the Prandtl number increases it. The suction of fluids and nanoparticles leads the fluid towards the stretching surface which causes an increase in the friction. However, with an increase in N_B and Le, the rates of mass transport increase as predicted in Table 6.

It is noticed that the Brownian motion raises the rate of mass transfer whereas the thermophoretic parameter is a decreasing function for the rate of heat transfer. The bulk amount of heat is generated inside the fluid due to the collision of the nanoparticles. Because of this fluid and the presence of base fluid, the particles start motion in a crisscross manner. The thermophoretic parameter generates large amount of heat due to particles collision which enlarges the temperature but declares an opposite behavior for heat transportation rate.

The density of the microorganisms on the surface of the sheet increases because of bioconvection which collect the fluid alongside the sheet. Table 7 elucidates the improvement in the density of the microbes on the surface of the

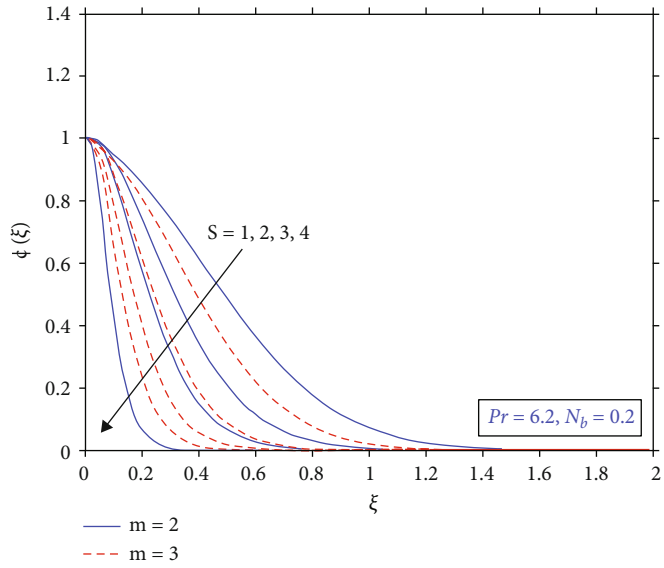

FIGURE 12: $\phi(\xi)$ for various values of S and m.

sheet when the values of Ω, Sc, and Pe increase. The transportation of mass toward fluid from sheet occurs if the fluid concentration at the surface is less than the concentration of nanoparticles. The low concentration on the sheet causes due to the improvement in (Nn_x). It is observed that the shear stress increases due to the porosity parameter whereas the motile microbes density raises due to the bioconvection parameters (e.g., Sc, Pe, and Ω) correspondingly.

The different properties of α describe the various cases such as shrinking and stretching of sheet is denoted by $\alpha > 0$ and $\alpha < 0$, respectively, and there is no boundary layer when $\alpha = 1$. The flow of planar stagnation point is associated with $\alpha = 0$. The behavior of temperature, velocity, and microbes density profiles for distinct α and m is depicted in Figures 3–5. In both the cases, shrinking $(\alpha = -1)$ and stretching $(\alpha = 0.5)$ of sheet, respectively, velocity of fluid increases. On the other hand, $\theta(\xi)$ and $G(\xi)$ are depressed with the effect of positive constant m. Figure 6 elucidates the consequences of injection/suction parameter S and porosity parameter P_0 on streamwise velocity $F'(\xi)$. The velocity $F'(\xi)$ elevates with an increase in P_0 and S.

Figure 7 evidently reveals that the Prandtl number reduces the temperature in the flow regime. The profile of temperature is shown in Figure 8 for different values of Ec and N_t. As we raise the values of both these parameters the temperature profile displays an increasing trend, the more heat transports in the fluid as the values of the Eckert number increase. This phenomenon affects the boundary layer thickness and causes an elevation in the temperature.

Thermophoretic and Brownian motions are accountable to the transport of nanoparticles. On the opposite, movement of mobile microbes powered by bioconvection is self-propelled. Therefore, the motion of tiny microbes is autonomous. The single-celled plants (phytoplankton) and single-celled green algae (chlamydomonas) can be analyzed as exemplary gyrotactic microbes. These are microscopic photosynthetic and green species that are useful to investigate the movement of microorganisms in fluid flows. These species can typically be contained in water or marine environment. The chlamydomonas and phytoplankton move upward due to gravitational force.

The effect of Lewis and Schmidt numbers for the bioconvection of motile organisms can be seen in Figure 9. A declining behavior in concentration profile is associated with the enlarging values of Le and Sc. The density of motile microbes depreciates while the viscous diffusion rate escalates due to increase in the bioconvection Lewis number.

Figure 10 clarifies that if we go on increasing the estimations of the microorganism's parameter and the bioconvective Peclet number; then, the profiles $G(\xi)$ are demoted. The bioconvection exists due to the up swimming of microorganisms on the upper surface of the fluid. In this problem, the viscous drag and the gravitational torques cause the motion of microorganisms. An increment in the values of the Peclet number Pe upsurges the rate of advective transport associated to the dispersion and, on the other side, the flux of self-swimming motile microbes increases rapidly. A deceleration in the thickness of the motile organisms near the surface occurs due to the production of the rate of swimming motile microbes by the bioconvection Peclet number in the fluid. The bioconvection parameters substantially affect the density of the motile microbes. Thermal or temperature inversion occurs when a layer of hot fluid settles over a layer of cooler fluid that lies near the boundary. Viscous dissipation effect causes thermal inversion (reversal) due to which more heat is generated near boundary. This is the reason that some graphs deviate (little bit) from the imposed boundary conditions. Figures 11 and 12 are portrayed against concentration to analyze the effects of Suction parameter and Lewis number. It is found here that the the effect of both these parameters, together with Brownian motion parameter and positive constant, is to reduce the concentration.

5. Conclusions

This paper discloses the novel study regarding the bioconvective flow of gyrotactic microorganisms and nanofluids through a porous media. The flow is taken over a nonlinear expanding/shrinking surface. Bioconvection flows of microbes together with nanoparticles have much useful employments in several fields of science and biotechnology. The system of flow model equations is initially simplified by the similarity transformations, and then, successive over relaxation scheme is used to solve the resultant system numerically. From the outcomes of this examination, it is interpreted that the usage of nanoparticles together with gyrotactic microorganisms drives the flow towards consistency and stability. The major outcomes are listed below:

(i) An increment in the motile microbes' parameter and bioconvection Schmidt number leads towards an enhancement in the diffusion rate of microorganisms. On the other hand, a decreasing trend in the density profiles of mobile microorganisms is observed due to an increase in bioconvection parameters

(ii) The viscous dissipation tends to decelerate the rate of heat transportation on the surface of sheet and elevates the temperature $\theta(\xi)$

(iii) The porosity parameter negligibly affects the density of motile microbes in the absence of viscous dissipation ($\mathrm{Ec} = 0$), while it substantially affects the density by increasing viscous dissipation

(iv) The dimensionless stream wise velocity profiles seem to be magnifying with an increase in the values of porosity, injection/suction, and stretching/shrinking parameters

Nomenclature

T_∞: Ambient temperature
T: Fluid temperature
k^*: Darcy permeability
N: Microorganism concentration
W_c: Cell swimming speed
ψ: Stream function
D_B: Brownian motion diffusivity
D_n: Diffusivity of microorganisms
τ: Heat capacity of nanofluid
Sh_x: Sherwood number
ρ: Fluid density
μ: Dynamic viscosity
D_T: Thermophoretic coefficient
K_c: Rate constant of chemical reaction
η: Similarity variable
θ: Dimensionless temperature
Nn_x: Density of motile microorganisms
u_w: Stretching velocity
Nu_x: Nusselt number
C_∞: Ambient concentration
m: Positive constant for nonlinear stretching sheet
a, c: Constants
$\tilde{\alpha}$: Thermal conductivity
u_e: Ambient velocity
N_∞: Ambient microorganisms concentration
C: Fuid concentration
C_{fx}: Skin friction
υ: Kinematics viscosity

Data Availability

The data used to obtain and finding this study are available from the corresponding author upon request.

Conflicts of Interest

The authors declare that they have no competing interests.

Authors' Contributions

All authors carried out the proofs and conceived of the study. All authors read and approved final form of the manuscript.

References

[1] N. Acharya, F. Mabood, S. A. Shahzad, and I. A. Badruddin, "Hydrothermal variations of radiative nanofluid flow by the influence of nanoparticles diameter and nanolayer," *International Communications in Heat and Mass Transfer*, vol. 130, article 105781, 2022.

[2] T. Salahuddin, N. Siddique, M. Khan, and Y.–. M. Chu, "A hybrid nanofluid flow near a highly magnetized heated wavy cylinder," *Alexandria Engineering Journal*, vol. 61, no. 2, pp. 1297–1308, 2022.

[3] A. Shafiq, Z. Hammouch, and T. N. Sindhu, "Bioconvective MHD flow of tangent hyperbolic nanofluid with newtonian heating," *International Journal of Mechanical Sciences*, vol. 133, pp. 759–766, 2017.

[4] A. Shafiq and T. N. Sindhu, "Statistical study of hydromagnetic boundary layer flow of Williamson fluid regarding a radiative surface," *Results in Physics*, vol. 7, pp. 3059–3067, 2017.

[5] M. Imran, U. Farooq, H. Waqas, A. E. Anqi, and M. R. Safaei, "Numerical performance of thermal conductivity in bioconvection flow of cross nanofluid containing swimming microorganisms over a cylinder with melting phenomenon," *Case Studies in Thermal Engineering*, vol. 26, article 101181, 2021.

[6] M. Bilal, A. Saeed, T. Gul, I. Ali, W. Kumam, and P. Kumam, "Numerical approximation of microorganisms hybrid nanofluid flow induced by a wavy fluctuating spinning disc," *Coatings*, vol. 11, no. 9, p. 1032, 2021.

[7] W. N. Mutuku and O. D. Makinde, "Hydromagnetic bioconvection of nanofluid over a permeable vertical plate due to gyrotactic microorganisms," *Computers & Fluids*, vol. 95, pp. 88–97, 2014.

[8] W. A. Khan, O. D. Makinde, and Z. H. Khan, "MHD boundary layer flow of a nanofluid containing gyrotactic microorganisms past a vertical plate with Navier slip," *International Journal of Heat and Mass Transfer*, vol. 74, pp. 285–291, 2014.

[9] T. L. Stewart and H. S. Fogler, "Biomass plug development and propagation in porous media," *Biotechnology and Bioengineering*, vol. 72, no. 3, pp. 353–363, 2001.

[10] M. Ramzan, J. D. Chung, and N. Ullah, "Radiative magnetohydrodynamic nanofluid flow due to gyrotactic microorganisms with chemical reaction and non-linear thermal radiation," *International Journal of Mechanical Sciences*, vol. 130, pp. 31–40, 2017.

[11] T. Chakraborty, K. Das, and P. K. Kundu, "Framing the impact of external magnetic field on bioconvection of a nanofluid flow containing gyrotactic microorganisms with convective boundary conditions," *Alexandria Engineering Journal*, vol. 57, no. 1, pp. 61–71, 2018.

[12] M. T. Sk, K. Das, and P. K. Kundu, "Multiple slip effects on bioconvection of nanofluid flow containing gyrotactic microorganisms and nanoparticles," *Journal of Molecular Liquids*, vol. 220, pp. 518–526, 2016.

[13] Z. Iqbal, Z. Mehmood, and E. N. Maraj, "Oblique transport of gyrotactic microorganisms and bioconvection nanoparticles with convective mass flux," *Physica E: Low-dimensional Systems and Nanostructures*, vol. 88, pp. 265–271, 2017.

[14] S. Atif, S. Hussain, and M. Sagheer, "Magnetohydrodynamic stratified bioconvective flow of micropolar nanofluid due to gyrotactic microorganisms," *AIP Advances*, vol. 9, no. 2, article 025208, 2019.

[15] N. Acharya, K. Das, and P. K. Kundu, "Framing the effects of solar radiation on magneto-hydrodynamics bioconvection nanofluid flow in presence of gyrotactic microorganisms," *Journal of Molecular Liquids*, vol. 222, pp. 28–37, 2016.

[16] H. Waqas, S. U. Khan, S. A. Shehzad, and M. Imran, "Radiative flow of Maxwell nanofluid containing gyrotactic microorganism and energy activation with convective Nield conditions," *Heat Transfer - Asian Research*, vol. 48, no. 5, pp. 1663–1687, 2019.

[17] S. Zuhra, S. N. Khan, M. Alam, S. Islam, and A. Khan, "Buoyancy effects on nanoliquids film flow through a porous medium with gyrotactic microorganisms and cubic autocatalysis chemical reaction," *Advances in Mechanical Engineering*, vol. 12, no. 1, Article ID 168781401989751, 2020.

[18] A. Aziz, W. A. Khan, and I. Pop, "Free convection boundary layer flow past a horizontal flat plate embedded in porous medium filled by nanofluid containing gyrotactic microorganisms," *International Journal of Thermal Sciences*, vol. 56, pp. 48–57, 2012.

[19] S. Shaw, S. S. Motsa, and P. Sibanda, "Magnetic field and viscous dissipation effect on bioconvection in a permeable sphere embedded in a porous medium with a nanofluid containing gyrotactic micro-organisms," *Heat Transfer - Asian Research*, vol. 47, no. 5, pp. 718–734, 2018.

[20] A. V. Kuznetsov, "Nanofluid bioconvection in porous media: oxytactic microorganisms," *Journal of Porous Media*, vol. 15, no. 3, pp. 233–248, 2012.

[21] A. Sarkar, K. Das, and P. K. Kundu, "On the onset of bioconvection in nanofluid containing gyrotactic microorganisms and nanoparticles saturating a non-Darcian porous medium," *Journal of Molecular Liquids*, vol. 223, pp. 725–733, 2016.

[22] R. M. M. Aurangzaib and A. J. Chamkha, "Flow of nanofluid containing gyrotactic microorganisms over static wedge in darcy-brinkman porous medium with convective boundary condition," *Journal of Porous Media*, vol. 21, no. 10, pp. 911–928, 2018.

[23] J. O. Kessler, "The external dynamics of swimming microorganisms," *Progress in Phycological Research*, vol. 4, pp. 257–307, 1986.

[24] A. Shahid, Z. Zhou, M. M. Bhatti, and D. Tripathi, "Magnetohydrodynamics nanofluid flow containing gyrotactic microorganisms propagating over a stretching surface by successive Taylor series linearization method," *Microgravity Science and Technology*, vol. 30, no. 4, pp. 445–455, 2018.

[25] S. Ahmad, M. Ashraf, and K. Ali, "Bioconvection due to gyrotactic microbes in a nanofluid flow through a porous medium," *Heliyon*, vol. 6, no. 12, article e05832, 2020.

[26] F. Mabood, S. Shateyi, M. M. Rashidi, E. Momoniat, and N. Freidoonimehr, "MHD stagnation point flow heat and mass transfer of Nanofluids in porous medium with radiation, viscous dissipation and chemical reaction," *Advanced Powder Technology*, vol. 27, no. 2, pp. 742–749, 2016.

[27] S. Ahmad, M. Ashraf, and K. Ali, "Nanofluid flow comprising gyrotactic microorganisms through a porous medium," *Journal of Applied Fluid Mechanics*, vol. 13, pp. 1539–1549, 2020.

[28] N. Z. Aini Mat, N. M. Arifin, R. M. Nazar, and F. Ismail, "Similarity solutions for the flow and heat transfer over a nonlinear stretching/shrinking sheet in a nanofluid," *AIP Conference Proceedings*, vol. 1450, pp. 165–172, 2012.

[29] S. Ahmad, K. Ali, M. Rizwan, and M. Ashraf, "Heat and mass transfer attributes of copper-aluminum oxide hybrid nanoparticles flow through a porous medium," *Case Studies in Thermal Engineering*, vol. 25, article 100932, 2021.

[30] S. Ahmad, K. Ali, and M. Ashraf, "MHD flow of Cu-Al_2O_3/water hybrid nanofluid through a porous media," *Journal of Porous Media*, vol. 24, no. 7, pp. 61–73, 2021.

[31] K. Ali, S. Ahmad, K. S. Nisar, A. A. Faridi, and M. Ashraf, "Simulation analysis ofMHDhybrid Cu⊠Al2O3/H2O nanofluid flow with heat generation through a porous media," *International Journal of Energy Research*, vol. 45, no. 13, pp. 19165–19179, 2021.

[32] S. Ahmad, K. Ali, S. Ahmad, and J. Cai, "Numerical study of lorentz force interaction with micro structure in channel flow," *Energies*, vol. 14, no. 14, p. 4286, 2021.

[33] S. Ahmad, M. Ashraf, K. Ali, and K. S. Nisar, "Computational analysis of heat and mass transfer in a micropolar fluid flow through a porous medium between permeable channel walls," *International Journal of Nonlinear Sciences and Numerical Simulation*, 2021.

[34] K. Zaimi, A. Ishak, and I. Pop, "Stagnation-point flow toward a Stretching/Shrinking sheet in a Nanofluid containing both Nanoparticles and gyrotactic microorganisms," *Journal of Heat Transfer*, vol. 136, no. 4, pp. 1–9, 2014.

[35] M. M. Rashidi, N. Freidoonimehr, A. Hosseini, O. A. Bég, and T. K. Hung, "Homotopy simulation of nanofluid dynamics from a non-linearly stretching isothermal permeable sheet with transpiration," *Meccanica*, vol. 49, no. 2, pp. 469–482, 2014.

[36] S. Ahmad, K. Ali, K. S. Nisar et al., "Features of Cu and TiO_2 in the flow of engine oil subject to thermal jump conditions," *Scientific Reports*, vol. 11, no. 1, p. 19592, 2021.

[37] S. Ahmad, K. Ali, A. A. Faridi, and M. Ashraf, "Novel thermal aspects of hybrid nanoparticles *Cu-TiO_2* in the flow of ethylene glycol," *International Communications in Heat and Mass Transfer*, vol. 129, article 105708, 2021.

[38] W. Jamshed, ,D. Baleanu, ,N. A. A. M. Nasir,,,,, et al., "The improved thermal efficiency of Prandtl-Eyring hybrid nanofluid via classical Keller box technique," *Scientific Reports*, vol. 11, no. 1, article 23535, 2021.